jove

Investigating Interactions Between Histone Modifying Enzymes and Transcription Factors *in vivo* by Fluorescence Resonance Energy Transfer

Mi Sa Vo Phan[1], **Phu Tri Tran**[1], **Vitaly Citovsky**[1]

[1] Department of Biochemistry and Cell Biology, State University of New York

Corresponding Author

Mi Sa Vo Phan
vpmisa@gmail.com

Citation

Vo Phan, M.S., Tran, P.T., Citovsky, V. Investigating Interactions Between Histone Modifying Enzymes and Transcription Factors *in vivo* by Fluorescence Resonance Energy Transfer. *J. Vis. Exp.* (188), e64656, doi:10.3791/64656 (2022).

Date Published

October 14, 2022

DOI

10.3791/64656

URL

jove.com/t/64656

Abstract

Epigenetic regulation of gene expression is commonly affected by histone modifying enzymes (HMEs) that generate heterochromatic or euchromatic histone marks for transcriptional repression or activation, respectively. HMEs are recruited to their target chromatin by transcription factors (TFs). Thus, detecting and characterizing direct interactions between HMEs and TFs are critical for understanding their function and specificity better. These studies would be more biologically relevant if performed *in vivo* within living tissues. Here, a protocol is described for visualizing interactions in plant leaves between a plant histone deubiquitinase and a plant transcription factor using fluorescence resonance energy transfer (FRET), which allows the detection of complexes between protein molecules that are within <10 nm from each other. Two variations of the FRET technique are presented: SE-FRET (sensitized emission) and AB-FRET (acceptor bleaching), in which the energy is transferred non-radiatively from the donor to the acceptor or emitted radiatively by the donor upon photobleaching of the acceptor. Both SE-FRET and AB-FRET approaches can be adapted easily to discover other interactions between other proteins *in planta*.

Introduction

Plant histone deubiquitinases play an important role in controlling gene expression by post-translational modification of histones, specifically by erasing their monoubiquitylation marks[1]. So far, OTLD1 is one of the only few plant histone deubiquitinases characterized at the molecular level in Arabidopsis[2,3]. OTLD1 removes monoubiquitin groups from the H2B histone molecules, thereby promoting the removal or addition of euchromatic acetylation and methylation modifications of H3 histones in the target gene chromatin[4,5]. Moreover, OTLD1 interacts with another chromatin-modifying enzyme, the histone lysine demethylase KDM1C, to affect transcriptional suppression of the target genes[6,7].

Most histone-modifying enzymes lack DNA binding capabilities, and thus cannot recognize their target genes directly. One possibility is that they cooperate

with DNA-binding transcription factor proteins which bind these enzymes and direct them to their chromatin targets. Specifically, in plants, several major histone-modifying enzymes (i.e., histone methyltransferases[8,9], histone acetyltransferases[10], histone demethylases[11], and Polycomb repressive complexes[12,13,14]) are known to be recruited by transcription factors. Consistent with this idea, recently, one possible mechanism for OTLD1 recruitment to the target promoters was proposed which is based on specific protein-protein interactions of OTLD1 with a transcription factor LSH10[15].

LSH10 belongs to a family of the plant ALOG (Arabidopsis LSH1 and Oryza G1) proteins that function as central developmental regulators[16,17,18,19,20,21,22]. The fact that the members of the ALOG protein family contain DNA binding motifs[23] and exhibit the capacities for transcriptional regulation[22], nuclear localization[19], and homodimerization[24] lends further support to the notion that these proteins, including LSH10, may act as specific transcription factors during epigenetic regulation of transcription. One of the main experimental techniques used to characterize the LSH10-OTLD1 interaction *in vivo* is fluorescence resonance energy transfer (FRET)[15].

FRET is an imaging technique for directly detecting close-range interactions between proteins within <10 nm from each other[25] inside living cells. There are two main variations of the FRET approach[26]: sensitized emission (SE-FRET) (**Figure 1A**) and acceptor bleaching (AB-FRET) (**Figure 1B**). In SE-FRET, the interacting proteins-one of which is tagged with a donor fluorochrome (e.g., green fluorescent protein, GFP) and the other with an acceptor fluorochrome (e.g., monomeric red fluorescent protein, mRFP[27,28])-non-radiatively transfer the excited state energy from the donor to the acceptor. Because no photons are emitted during this transfer, a fluorescent signal is produced that has a radiative emission spectrum similar to that of the acceptor. In AB-FRET, protein interactions are detected and quantified based on elevated radiative emission of the donor when the acceptor is permanently inactivated by photobleaching, and thus is unable to receive the non-radiative energy transferred from the donor (**Figure 1**). Importantly, the subcellular location of the FRET fluorescence is indicative of the localization of the interacting proteins in the cell.

The ability to deploy FRET in living tissues and determine the subcellular localization of the interacting proteins simultaneously with detecting this interaction per se, makes FRET the technique of choice for studies and initial characterization of protein-protein interactions *in vivo*. A comparable *in vivo* fluorescence imaging methodology, bimolecular fluorescence complementation (BiFC)[29,30,31,32], is a good alternative approach, although, unlike FRET, BiFC may produce false positives due to spontaneous assembly of the autofluorescent BiFC reporters[33], and quantification of its data is less precise.

This article shares the successful experience in implementing both SE-FRET and AB-FRET techniques and presents a protocol for their deployment to investigate the interactions between OTLD1 and LSH10 in plant cells.

Protocol

Nicotiana benthamiana, *Agrobacterium tumefaciens* strain EHA105, or GV3101 were used for the present study.

1. FRET vector construction

1. Select fluorescent tags for the donor/acceptor FRET pair.

1. Use EGFP from pPZP-RCS2A-DEST-EGFP-N1[15,28] (see **Table of Materials**) to generate the donor vector.
2. Use mRFP from pPZP-RCS2A-DEST-mRFP-N1 (see **Table of Materials**) to generate the acceptor vector.

2. Generate the donor/acceptor FRET constructs using a site-specific recombination cloning technique[34], such as the Gateway recombination cloning system[35].
   1. Amplify the coding sequences of the proteins of interest[36] (i.e., the Arabidopsis *OTLD1* and *LSH10*)[15].
      NOTE: It is also a good idea to utilize a negative control that represents a homolog of one of the interacting proteins but is not expected to exhibit interaction; the OTLD1-LSH10 interaction study employs a homolog of LSH10, LSH4, that does not recognize OTLD1. OTLD1, LSH10, and LSH4 cDNAs are amplified by PCR using primers listed in **Table 1**.
   2. Clone *OTLD1, LSH10*, and *LSH4* into the entry vector pDONR207 by the site-specific recombination cloning technique[34].
   3. Use the Gateway LR Clonase II (see **Table of Materials**) to transfer *LSH10* and *LSH4* from pDONR207 into the binary destination vector pPZP-RCS2A-DEST-EGFP-N1 to generate the binary donor constructs p35S::LSH10-GFP (tested construct) and p35S::LSH4-GFP (negative control).
   4. Use the same commercially available enzyme (step 1.2.3) to transfer *OTLD1* from pDONR207 into the binary destination vector pPZP-RCS2A-DEST-mRFP-N1 to generate the binary acceptor construct p35S::OTLD1-mRFP (tested construct).
   5. PCR-amplify[36] mRFP from pPZP-RCS2A-DEST-mRFP-N1 using primers listed in **Table 1**, clone it by the recombination cloning technique into pDONR207, and then use LR Clonase II to transfer mRFP into pPZP RCS2A-DEST-EGFP-N1 to generate the binary fusion construct p35S::mRFP-GFP (positive control).

3. Perform transformation of the donor and acceptor constructs into Agrobacterium.
   1. Add 1 µg of each plasmid from steps 1.2.3-1.2.5 to 100 µL of the culture of competent cells of *Agrobacterium tumefaciens* strain EHA105 or GV3101, prepared using standard protocols[37] or obtained commercially, and incubate at 37 °C for 5 min.
   2. Add 1 mL of LB medium (1% tryptone, 0.5% yeast extract, and 1% NaCl; see **Table of Materials**) to the competent cell mixture and agitate at 200 rpm and 28° C for 1.5 h. Collect the cells by centrifugation at 3,000 × *g* for 1 min at room temperature.
   3. Resuspend the cells in 0.1 mL of LB medium by pipetting and spread them on LB agar supplemented with the appropriate antibiotics (e.g., 0.01% spectinomycin and 0.005% rifampicin; see **Table of Materials**). Grow at 28 °C for 2 days.
   4. Pick individual colonies and inoculate each of them separately into 1 mL of LB broth supplemented with the appropriate antibiotics.
   5. Grow the cells at 28 °C for 24 h and transfer 0.2 mL of the culture into a new tube. Collect the cells

by centrifugation at 10,000 × *g* for 30 s at room temperature.

6. Extract plasmid DNA by a standard protocol for isolating plasmids from Agrobacterium cells[38] and resuspend the extracted DNA in 30 µL of water. To identify the colonies harboring the desired plasmids, use 2 µL of the DNA preparation as a template for PCR with gene-specific primers listed in **Table 1**. Mix 0.7 mL of the identified culture with 0.3 mL of glycerol and store at -80 °C.

2. Agroinfiltration

1. Grow *Nicotiana benthamiana* plants.

   NOTE: Throughout the entire experiment, all plants must be healthy.

   1. Sow and grow *N. benthamiana* seeds in a pot containing wet soil at a high density.
   2. Keep the planted seeds in a growth chamber set at 23 °C with 16 h of light and 8 h of dark cycle with 150-170 µmol/m^2s light intensity until the diameter of the euphyll reaches 0.5 cm.
   3. Transfer the seedlings to larger pots and allow them to grow in the same chamber with the same parameters.

      NOTE: Plants are ready for agroinfiltration when their largest leaves are 5-7 cm in diameter, usually within 4-5 weeks. In smaller plants that are too young, the effects of agroinfiltration will be too severe for the FRET analysis.

2. Prepare bacterial cells for agroinfiltration.

   1. Grow each Agrobacterium colony containing the FRET constructs overnight in 5 mL of LB medium supplemented with the appropriate antibiotics (step 1.3.3) and 150 µM acetosyringone at 28 °C (see **Table of Materials**).
   2. Centrifuge the cells at 3,000 × *g* for 5 min at room temperature.
   3. Resuspend the cells in agroinfiltration buffer (10 mM $MgCl_2$, 10 mM MES pH 5.6, 150 µM acetosyringone) to OD_{600} = 0.5.
   4. Combine the resuspended cells at a 1:1 v/v ratio between cells harboring the appropriate constructs (step 2.2.5).
   5. For the double-construct agroinfiltrations, mix the aliquots of two cultures and, for single-construct agroinfiltrations, mix the aliquots of the same culture:
      1. Tested proteins: OTLD1-mRFP + LSH10-GFP (bacteria harboring the p35S::OTLD1-mRFP and p35S::LSH10-GFP constructs).
      2. Negative control: OTLD1-mRFP + LSH4-GFP (bacteria harboring the p35S::OTLD1-mRFP and p35S::LSH4-GFP constructs).
      3. Negative control: LSH10-GFP + free mRFP (bacteria harboring the p35S::LSH10-GFP and pPZP-RCS2A-DEST-mRFP-C1 constructs).
      4. Positive control: mRFP-GFP (bacteria harboring the p35S::mRFP-GFP construct).
   6. Incubate the cells at 28 °C for 0.5-1 h.

3. Perform agroinfiltration.

   1. Load the bacterial culture into a 1 mL needleless syringe.
   2. Gently but firmly press the nozzle of the syringe against the abaxial side of the fully expanded *N.*

benthamiana leaves while holding the leaf with a gloved finger on the adaxial side.

3. Infiltrate up to four spots on a leaf, three leaves per plant, two or three plants for each bacterial culture. Change gloves between samples to prevent cross-contamination.

4. Maintain the agroinfiltrated plants in the same growth chamber under the same conditions, as described in step 2.1.2, for 24 h to 36 h. Do not keep the agroinfiltrated plants for longer than 36 h, as this will reduce the fluorescence signal.

3. Confocal microscopy

1. Prepare microscope slides for fluorescence visualization.
    1. After 24-36 h of the infiltration, use a razor blade to cut each agroinfiltrated leaf into small pieces (2 mm x 4 mm) between the veins.
    2. Place the leaf pieces on a glass slide with the abaxial leaf surface facing up. Place a drop of water on the leaf pieces and cover them with the cover glass. Slightly tap the cover glass to remove air bubbles.
    3. Turn on the microscope and laser (see **Table of Materials**). Place the slide into the microscope stage holder for imaging under the specific FRET parameters (steps 3.2 and 3.3).
    4. Begin the observations using a 10x objective lens to identify cells that exhibit both the GFP and mRFP signals, and then use a 40x objective lens for subsequent detailed observations.
    NOTE: Importantly, SE-FRET and AB-FRET usually are performed on the same tissue sample, allowing the use of the same channel settings (step 3.2) except for the FRET channel, which is toggled on/off for the SE-FRET and AB-FRET observations, respectively (steps 3.2.2.3 and 3.3.1).
2. Set up the parameters for SE-FRET (**Figure 1A**).
    1. Open the Multi-Dimensional Acquisition (MDA) tool.
    2. Establish a set of three confocal channels in the same field of view (**Supplementary Figure 1**).
        1. Set the donor channel (the GFP channel) for excitation and emission of the donor fluorochrome with the 405 nm excitation laser and 400-597 nm emission filter.
        2. Set the acceptor channel (the mRFP channel) for excitation and emission of the acceptor fluorochrome with the 561 nm excitation laser and 400-597 nm emission filter.
        NOTE: The emission filter for mRFP was set at 400-597 nm to separate the mRFP signal from the FRET signal at 597-617 nm (step 3.2.2.3) and, therefore, reduce the FRET-independent mRFP emission.
        3. Set the FRET channel for excitation of the donor and emission of the acceptor fluorochromes with the 405 nm excitation laser and 597-617 nm emission filter.
    3. Set the donor excitation intensity at a minimum level to observe FRET while avoiding photobleaching, reducing the SE-FRET efficiency.
    NOTE: This excitation intensity is experimentally selected before conducting the FRET procedure to avoid photobleaching. It varies depending on leaf thickness, age, and time after overexpression.
    4. Excite the donor and scan for cells containing the acceptor's expected fluorescence signal.

5. Select the region that contains the fluorescence signal of interest.

6. Acquire a SE-FRET image sequence by pressing the **Snap** button.

    1. Image 10-15 cells expressing the mRFP-GFP construct (positive control) first; adjust the focus, zoom, and smart gain parameters to focus on the area of interest to be captured (**Supplementary Figure 2**).

    2. Using the same settings, image 10-15 cells, each expressing OTLD1-mRFP, free mRFP, LSH10-GFP, or LSH4-GFP separately.
    NOTE: These images are acquired by the "PixFRET" plug-in of ImageJ (see **Table of Materials**), which was used for the FRET data analyses (step 3.4.1) to determine the spectral bleed-through (SBT) values for the acceptors and the donors; these images are used by the software to generate the SE-FRET images for the OTLD1-mRFP + LSH10-GFP, OTLD1-mRFP + LSH4-GFP, and LSH10-GFP + free mRFP protein pairs (step 3.2.6.3).

    3. Also, using the same settings, image 10-15 cells co-expressing OTLD1-mRFP + LSH10-GFP, OTLD1-mRFP + LSH4-GFP, and LSH10-GFP + free mRFP protein pairs.

3. Set up parameters for AB-FRET (**Figure 1B**).

    1. Utilize the donor and acceptor channel parameters set for SE-FRET (step 3.2.2) but turn off the FRET channel.

    2. Set the parameters for photobleaching of the acceptor (mRFP) (**Supplementary Figure 3**).

        1. Ensure that bleaching starts after five images. Allow 200 iterations for each area bleach. Keep 100% laser intensity at 561 nm.

        2. Maintain a bleaching duration of 45 s. Ensure a scan speed of 512 x 512 pixels at 400 Hz.

    3. Draw the region of the cell to be bleached; for example, for nuclear interactions, regions of interest are drawn around the entire area of the cell nucleus[39].

    4. Activate bleaching by pressing the **Start experiment** button; activating this function will perform the photobleaching and acquire the AB-FRET image sequence.

4. Analyze the FRET data.

    1. For analyzing SE-FRET data, use the "PixFRET" plug-in for the ImageJ software to generate corrected images of the SE-FRET efficiency after subtracting SBT[40] (step 3.2.6.2).

    2. For analyzing the AB-FRET data, calculate %AB-FRET as the percent increase in GFP emission after mRFP photobleaching using the following formula[41]: %AB-FRET = [(GFPpost - GFPpre) / GFPpre] x 100, where GFPpost is GFP emission after mRFP photobleaching, and GFPpre is GFP emission before mRFP photobleaching.

    3. When reviewing the FRET images, pay attention to the subcellular localization of the FRET signal.
    NOTE: In many cases, these cellular compartments (e.g., nucleus, chloroplasts, ER, etc.) can be easily identified and, as an additional benefit of the FRET technique, provide important clues to the biological function of the interacting proteins.

Representative Results

Figure 2 illustrates the typical results of a SE-FRET experiment, in which the cell nuclei were simultaneously recorded in three channels (i.e., donor GFP, acceptor mRFP, and SE-FRET). These data were used to generate images of SE-FRET efficiency coded in a pseudo-color scale. On this scale, the transition from blue to red corresponds to an increase in FRET efficiency, a measure of protein-protein proximity from 0% to 100%. In this representative experiment, the SE-FRET signal was recorded in the cell nucleus, and its intensity following the coexpression of LSH10 and OTLD1 was comparable to that observed after the expression of the mRFP-GFP (i.e., positive control). No SE-FRET was observed in negative controls (i.e., coexpression of OTLD1-mRFP and LSH4-GFP or free mRFP and LSH10-GFP).

The LSH10-OTLD1 interactions were quantified using AB-FRET. To this end, the donor GFP fluorescence was recorded in the cell nucleus before and after the photobleaching of the acceptor mRFP as photobleaching time series of donor and acceptor fluorescence measurements (**Supplementary Figure 4**). The images of the recorded cell nuclei were presented in pseudo-color to quantify the change in GFP fluorescence. **Figure 3** shows that the LSH10-GFP/OTLD1-mRFP coexpression resulted in an increased GFP donor fluorescence after the mRFP acceptor was photobleached and lost its ability to fluoresce. A similar increase in the donor fluorescence was observed in the mRFP-GFP positive control but not in the negative controls of LSH4-GFP/OTLD1-mRFP or LSH10-GFP/mRFP coexpression, whereas the acceptor fluorescence was inactivated in all photobleaching experiments. **Figure 4** shows the quantitative analysis of the AB-FRET data, demonstrating the statistically significant increase in the donor fluorescence (%AB-FRET) of approximately 13% after coexpressing LSH10 and OTLD1. The positive mRFP-GFP control produced %AB-FRET of approximately 30%, whereas the negative controls produced no %AB-FRET. Both SE-FRET and AB-FRET images showed the FRET signal in the cell nucleus, consistent with the subcellular localization expected for the transcription factor-histone-modifying enzyme complexes as well as for the nucleocytoplasmic nature of the GFP/mRFP proteins[34] (**Figure 2** and **Figure 3**).

In summary, the representative data show that this FRET protocol can be used to demonstrate and quantify interactions between histone-modifying enzymes and transcription factors and determine their subcellular localization in living plant cells.

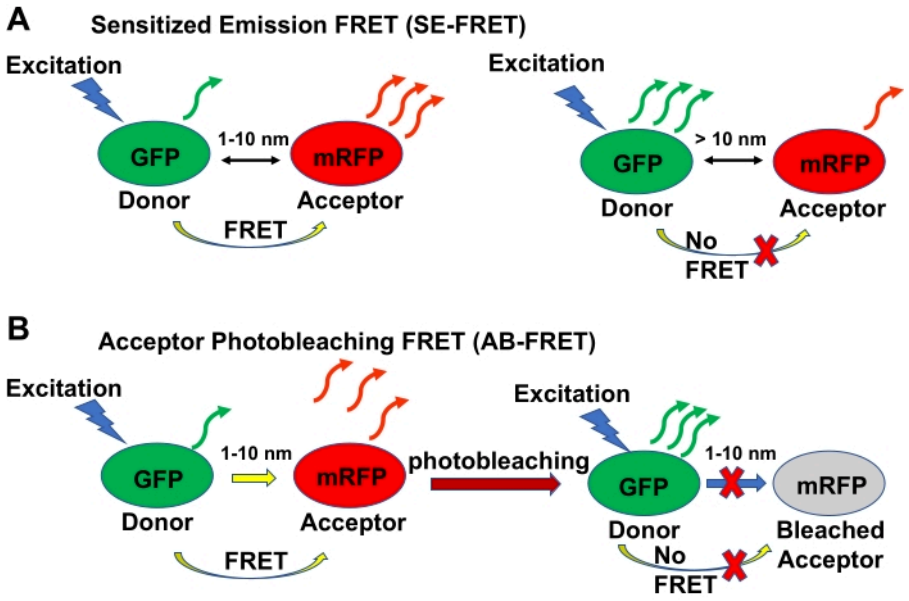

Figure 1: Schematic summary of the SE-FRET and AB-FRET techniques. (**A**) The basic principle of SE-FRET. One of the tested proteins is tagged with GFP, which acts as a donor fluorochrome, and the other with mRFP, which acts as an acceptor fluorochrome. The donor molecule is excited, and the acceptor emission is recorded. If the tested proteins interact with each other such that they are positioned within 10 nm of each other, the energy from the excited donor is transferred non-radiatively to the acceptor, which then becomes excited and emits fluorescence in the FRET emission channel. If no interaction occurs, no energy is transferred from the donor to the acceptor, and no FRET emission by the acceptor is detected. (**B**) The basic principle of AB-FRET. The tested proteins are tagged as described in (**A**) for SE-FRET. The donor molecule is excited, and if the interaction between the tested proteins occurs, the donor excites the acceptor in a non-radiative fashion, resulting in FRET. Then, the acceptor is permanently inactivated by photobleaching, thereby losing its ability to accept non-radiative energy from the donor and emit the FRET fluorescence in the FRET emission channel; the fluorescence emitted by the donor, on the other hand, is increased because the donor loses less energy by the non-radiative transfer. Please click here to view a larger version of this figure.

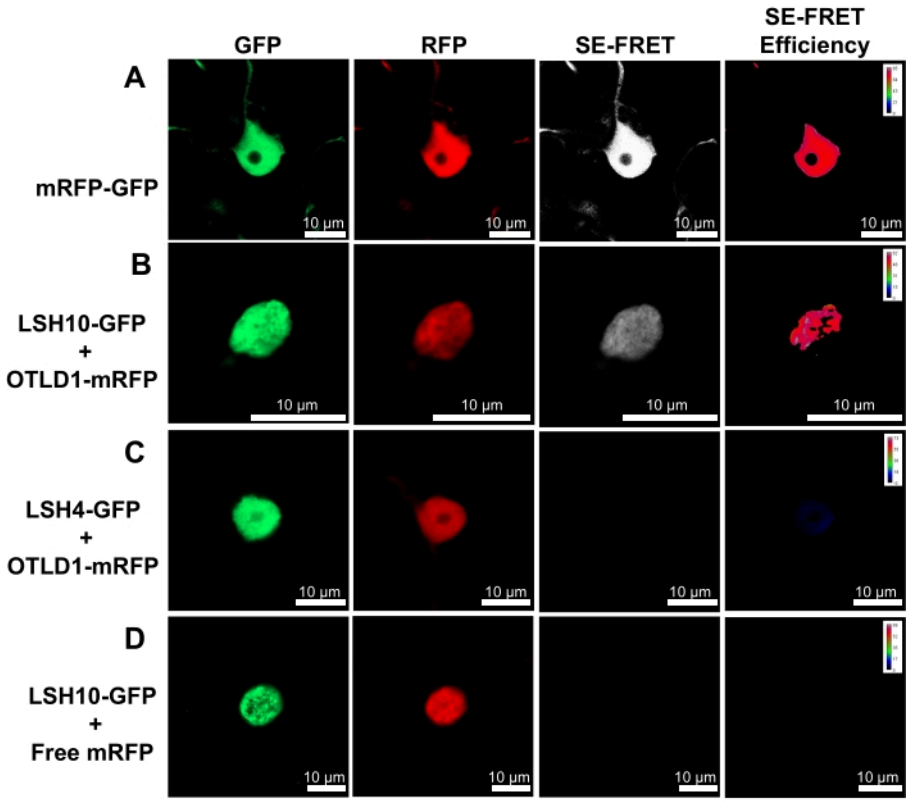

Figure 2: Specific interaction of LSH10 with OTLD1 in *N. benthamiana* leaves detected by SE-FRET. Images from three detection channels (donor, acceptor, and SE-FRET) are shown for the indicated protein combinations. The SE-FRET efficiency images were calculated by the subtraction of spectral bleed-through (SBT) and are shown in pseudo-color, with the colors red and blue signifying the highest and the lowest signal, respectively. (**A**) High SE-FRET efficiency signal produced by the mRFP-GFP positive control. (**B**) Positive SE-FRET efficiency signal produced by the interacting LSH10-GFP and OTLD1-mRFP proteins. (**C**) Coexpression of the negative control protein LSH4-GFP and OTLD1-mRFP produced no SE-FRET efficiency signal. (**D**) Coexpression of the negative control-free mRFP protein and LSH10-GFP produced no SE-FRET efficiency signal. Scale bars = 10 µm. Please click here to view a larger version of this figure.

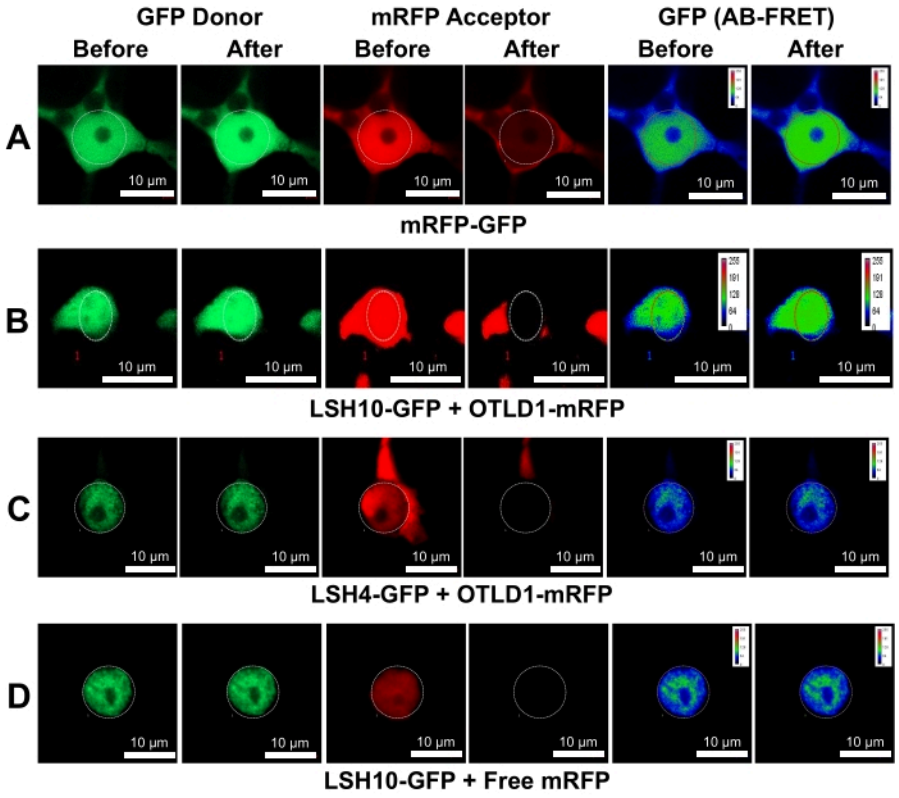

Figure 3: Specific interaction of LSH10 with OTLD1 in *N. benthamiana* leaves detected by AB-FRET. Images from two detection channels (donor and acceptor) before and after photobleaching are shown for the indicated protein combinations. The circle indicates the photobleached region. AB-FRET, visualized as an increase in GFP fluorescence after mRFP photobleaching, is displayed using pseudo-color with the colors red and blue, signifying the highest and lowest signal, respectively. (**A**) An increase in the GFP donor fluorescence produced by the mRFP-GFP positive control. (**B**) An increase in the GFP donor fluorescence produced by the interacting LSH10-GFP and OTLD1-mRFP proteins. (**C**) Coexpression of the negative control protein LSH4-GFP and OTLD1-mRFP produced negligible changes in the GFP donor fluorescence. (**D**) Coexpression of the negative control free mRFP protein and LSH10-GFP produced negligible changes in the GFP donor fluorescence. Scale bars = 10 µm. Please click here to view a larger version of this figure.

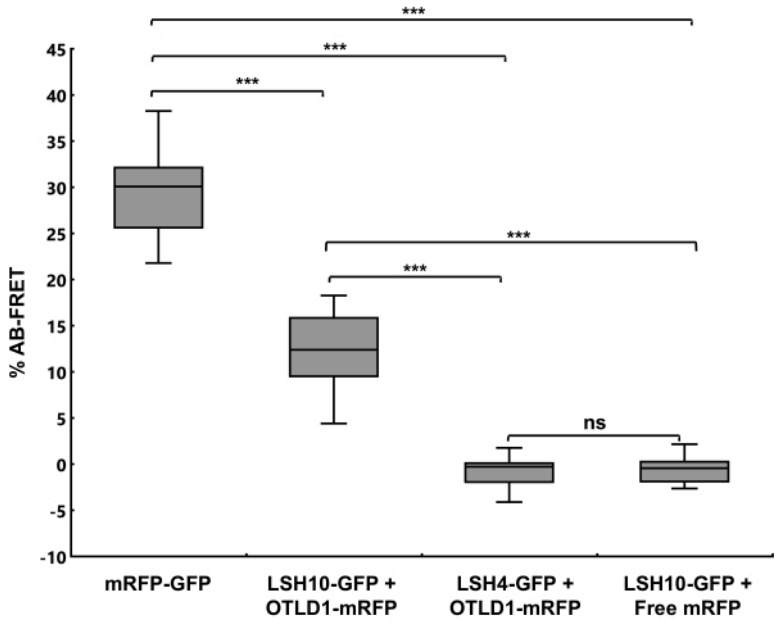

Figure 4: A Quantification of AB-FRET. The percentage increase in the GFP donor fluorescence after mRFP photobleaching (%AB-FRET) is shown for the indicated protein combinations. Error bars represent the mean for n = 13 cells for each measurement. The two-tailed t-test determined that differences between mean values are statistically significant for the p-values *$p < 0.05$, **$p < 0.01$, and ***$p < 0.001$; $p \geq 0.05$ are not statistically significant (ns). Please click here to view a larger version of this figure.

Primer name	Sequence (5' to 3')	Purpose
OTLD1 Fw	ggggacaagtttgtacaaaaaagcaggctcaatgactcggattttggttcaaag	Amplify *OTLD1* from cDNA
OTLD1 Rv	ggggaccactttgtacaagaaagctgggtgttccgtggctttgcctttgcgtc	Amplify *OTLD1* from cDNA
LSH10 Fw	ggggacaagtttgtacaaaaaagcaggctcaatgtcctctccaagagaaagagg	Amplify *LSH10* from cDNA
LSH10 Rv	ggggaccactttgtacaagaaagctgggtgatgtcaacagagactaaagaaac	Amplify *LSH10* from cDNA
LSH4 Fw	ggggacaagtttgtacaaaaaagcaggctcaatggatcatatcatcggctttatg	Amplify LSH4 from cDNA
LSH4 Rv	ggggaccactttgtacaagaaagctgggtgattagggctacttgaaatcgcc	Amplify *LSH4* from cDNA
mRFP Fw	ggggacaagtttgtacaaaaaagcaggctcaatggcctcctccgaggacgt	Amplify mRFP from pPZP-RCS2A-DEST-mRFP-N1
mRFP Rv	ggggaccactttgtacaagaaagctgggtgttggagatctgcggccgcgg	Amplify mRFP from pPZP-RCS2A-DEST-mRFP-N1
AttL1	tcgcgttaacgctagcatggatctc	Confirm sequences in pDONR207 by PCR and DNA sequencing
AttL2	gtaacatcagagattttgagacac	Confirm sequences in pDONR207 by PCR and DNA sequencing
AttB1 Fw	ggggacaagtttgtac aaaaaagcaggct	Confirm sequences in destination vectors by PCR and DNA sequencing
AttB2 Rv	ggggaccactttgta caagaaagctgggt	Confirm sequences in destination vectors by PCR and DNA sequencing
35S Promoter Fw	ctatccttcgcaagacccttc	Confirm sequences in destination vectors by PCR

Table 1: Primers for cloning and confirming the cloned sequences in pDONOR207 and destination vectors. Fw, forward primers; Rv, reverse primers.

Supplementary Figure 1: Setting parameters for confocal channels. (**A**) Screenshot for the excitation and emission parameter setup for the donor channel (GFP). (**B**) Screenshot for the excitation and emission parameter setup for the acceptor channel (mRFP). (**C**) Screenshot for the excitation and emission parameter setup for the FRET channel. Please click here to download this File.

Supplementary Figure 2: Adjusting parameters for the acquisition of SE-FRET images of the sample of interest. (**A**) Screenshot for the scan area parameter setup (i.e., image size, scan speed, direction, and averaging). (**B**) Screenshot for the GFP channel parameter setup (i.e., laser, pinhole, master gain, and digital gain). (**C**) Screenshot for the mRFP channel parameter setup (i.e., laser, pinhole, master gain, and digital gain). (**D**) Screenshot for the FRET channel parameter setup (i.e., laser, pinhole, master gain, and digital gain). Please click here to download this File.

Supplementary Figure 3: Setting parameters for the acceptor photobleaching. (**A**) Screenshot for the scan area parameter setup (i.e., image size, scan speed, direction, and averaging). (**B**) Screenshot for the time series and time bleaching parameter setup. Please click here to download this File.

Supplementary Figure 4: Time series of the donor and acceptor fluorescence measurements during AP-FRET. The kinetics of the acceptor (mRFP) and donor (GFP) fluorescence was determined for the indicated samples before, during, and after the photobleaching period. (**A**) Positive mRFP-GFP control. (**B**) LSH10-GFP + OTLD1-mRFP. (**C**) Negative LSH4-GFP + OTLD1-mRFP control. (**D**) Negative LSH10-GFP + Free mRFP control. Yellow lines indicate the photobleaching time period. White curves plot the measurements of the fluorescence kinetics. In each panel, the upper and the lower images show the kinetics of the acceptor (mRFP) and donor (GFP) fluorescence, respectively. Note that, naturally, the GFP fluorescence often decreases over time because the laser gradually photobleaches the GFP itself. Please click here to download this File.

Discussion

This FRET protocol is simple and easy to reproduce; it also requires minimal supply investment and utilizes standard equipment for many modern laboratories. Specifically, five main technical features distinguish the versatility of this procedure. First, the FRET constructs are generated using site-specific recombination, a cloning approach that is easy to use, produces accurate results, and saves time compared to traditional restriction enzyme-based cloning. Second, *N. benthamiana* plants are simple to grow, produce relatively large amounts of tissue and are available in most laboratories. Third, agroinfiltration results in transient expression of the delivered constructs and, thus, generates data within a relatively short period of time (i.e., 24-36 h) compared to the months required to produce transgenic plants. Fourth, the ability to deliver different combinations of the constructs of interest by co-agroinfiltration allows testing of interactions between any proteins. Lastly, both SE-FRET and AB-FRET can be performed sequentially on the same tissue sample only by turning on/off one of the laser channel settings. It should be noted, however, that microbombardment delivery[42] can be used as an alternative approach for construct delivery into the plant tissues instead of agroinfiltration; in this case, the use of binary vectors required for agroinfiltration is unnecessary.

One critical step of this protocol is properly selecting the donor and acceptor fluorochrome pair to optimize the FRET efficiency. The following three factors should be considered: (1) the donor emission spectrum needs to maximally overlap the acceptor absorption spectrum to maximize the amount of transferred energy; (2) the donor's and acceptor's emission spectra must be sufficiently different to be distinguished from each other and to minimize SBT of the signal detected by microscopy; (3) the acceptor must have minimal direct

excitation at the absorbance maximum of the donor to minimize excitation of the acceptor during excitation of the donor. Common donor/acceptor FRET pairs used are cyan/yellow and green/red fluorescent proteins (i.e., CFP/YFP and GFP/mRFP, respectively). This protocol utilizes the GFP/mRFP pair because it is suitable for live cell imaging and, unlike the cyan/yellow FRET pairs, exhibits low phototoxicity and low photobleaching[43]. Conveniently, the translational fusion between the FRET pair (i.e., mRFP-GFP) serves as an ideal FRET positive control.

Another critical step is the selection of the appropriate negative controls. For example, in the case of the LSH10-OTLD1 interaction, the FRET analysis must always include the expression of OTLD1 alone, LSH10 alone, and coexpression of OTLD1 and LSH10 with proteins for which the interaction is not expected (i.e., LSH4 and free mRFP, respectively). In terms of the negative controls' choice, FRET experiments can follow the guidelines on best practices for the use of the BiFC technique[44], another fluorescence imaging-based approach adapted for the detection of protein interactions in living plant cells[29,30,31,32].

Finally, a factor affecting the FRET experimentation is common to all experiments in living plant tissues, and it derives from the varying physiological conditions of the plant, in general, and the agroinfiltrated transformed cells, in particular, even when maintained under control growth conditions. This physiological variability can contribute to a certain variability of the FRET data between individual experiments, plants, and even leaves. Thus, it is important to use at least two plants and three leaves per plant for each experiment and to select mature, fully expanded leaves for agroinfiltration, as they yield better images.

As with all experimental methodologies, FRET has its technical and usage-based limitations. One such limiting factor is the nature of the autofluorescent tag and its location within the protein of interest (e.g., at the amino- or carboxyl-terminus), which may interfere with the biological properties of this protein, such as its native pattern of subcellular localization or the ability to recognize its natural interactors. Before tagging, each protein of interest must be analyzed, to the extent possible, for its structural features that may be compromised by tagging. In many cases, however, the tagging parameters must be determined empirically based on the known activities of the protein of interest. Another major limitation is the relative technical sophistication of FRET, which requires using confocal microscopy with the appropriate hardware and software. Unlike several other protein interaction methods, such as the yeast two-hybrid system (Y2H)[45,46,47], FRET is unsuitable for identifying protein interactions by screening expression libraries, especially high-throughput screens[48]. In addition, as most assays performed *in vivo*, FRET is not a biochemically pure system, and thus, it does not detect the potential involvement of other unknown cellular factors in the interaction.

The significance of FRET with respect to other assays of protein interactions lies in its detection of short-distance interactions, reducing the chances for false-positive results, applicability for deployment *in vivo* in a variety of cells, tissues, and organisms (including plants), and detection of the subcellular localization of the interacting proteins. Many of these characteristics of FRET are found in other *in vivo* approaches, such as split-luciferase[49,50] or BiFC[29,30,31,32,33], among which BiFC is perhaps the most commonly used. Another widely used interaction assay is Y2H[45,46,47]; however, outside of yeast biology

research, this assay utilizes a heterologous experimental system, prone to false positives, and its findings require confirmation by another technique. A conceptual variation of Y2H is a split-ubiquitin assay which is better suited for detecting interactions between membrane proteins[51,52] and which exhibits limitations relative to FRET that is similar to Y2H. Finally, protein interactions can be detected by co-immunoprecipitation (co-IP), which applies to detection in a complex environment of cell extracts as well as in precisely defined *in vitro* reactions[53,54,55]; in our experience, co-IP is most useful as an alternative and independent method to confirm data obtained using the fluorescence-based *in vivo* approaches.

Whereas this specific FRET protocol was developed to study the interactions between plant transcription factors and histone-modifying enzymes, it can be used to discover and characterize interactions between many other classes of proteins *inplanta*.

Disclosures

No conflicts of interest were declared.

Acknowledgments

The work in V.C.'s laboratory is supported by grants from NIH (R35GM144059 and R01GM50224), NSF (MCB1913165 and IOS1758046), and BARD (IS-5276-20) to V.C.

References

1. March, E., Farrona, S. Plant deubiquitinases and their role in the control of gene expression through modification of histones. *Frontiers in Plant Science.* **8**, 2274 (2018).
2. Isono, E., Nagel, M. K. Deubiquitylating enzymes and their emerging role in plant biology. *Frontiers in Plant Science.* **5**, 56 (2014).
3. Feng, J., Shen, W. H. Dynamic regulation and function of histone monoubiquitination in plants. *Frontiers in Plant Science.* **5**, 83 (2014).
4. Keren, I., Citovsky, V. Activation of gene expression by histone deubiquitinase OTLD1. *Epigenetics.* **12** (7), 584-590 (2017).
5. Keren, I., Citovsky, V. The histone deubiquitinase OTLD1 targets euchromatin to regulate plant growth. *Science Signaling.* **9** (459), ra125 (2016).
6. Krichevsky, A., Lacroix, B., Zaltsman, A., Citovsky, V. Involvement of KDM1C histone demethylase-OTLD1 otubain-like histone deubiquitinase complexes in plant gene repression. *Proceedings of the National Academy of Sciences.* **108** (27), 11157-11162 (2011).
7. Keren, I., Lapidot, M., Citovsky, V. Coordinate activation of a target gene by KDM1C histone demethylase and OTLD1 histone deubiquitinase in *Arabidopsis. Epigenetics.* **14** (6), 602-610 (2019).
8. Kim, S. Y., Michaels, S. D. *SUPPRESSOR OF FRI 4* encodes a nuclear-localized protein that is required for delayed flowering in winter-annual *Arabidopsis. Development.* **133** (23), 4699-4707 (2006).
9. Kim, S., Choi, K., Park, C., Hwang, H. J., Lee, I. *SUPPRESSOR OF FRIGIDA4*, encoding a C2H2-type zinc finger protein, represses flowering by transcriptional activation of *Arabidopsis FLOWERING LOCUS C. The Plant Cell.* **18** (11), 2985-2998 (2006).
10. Sridhar, V. V., Surendrarao, A., Gonzalez, D., Conlan, R. S., Liu, Z. Transcriptional repression of target genes by

LEUNIG and SEUSS, two interacting regulatory proteins for *Arabidopsis* flower development. *Proceedings of the National Academy of Sciences.* **101** (31), 11494-11499 (2004).

11. Ning, Y. Q. et al. Two novel NAC transcription factors regulate gene expression and flowering time by associating with the histone demethylase JMJ14. *Nucleic Acids Research.* **43** (3), 1469-1484 (2015).
12. Hecker, A. et al. The *Arabidopsis* GAGA-binding factor BASIC PENTACYSTEINE6 recruits the POLYCOMB-REPRESSIVE COMPLEX1 component LIKE HETEROCHROMATIN PROTEIN1 to GAGA DNA motifs. *Plant Physiology.* **168** (3), 1013-1024 (2015).
13. Xiao, J. et al. *Cis* and *trans* determinants of epigenetic silencing by Polycomb repressive complex 2 in *Arabidopsis. Nature Genetics.* **49** (10), 1546-1552 (2017).
14. Yuan, W. et al. A *cis* cold memory element and a *trans* epigenome reader mediate Polycomb silencing of *FLC* by vernalization in *Arabidopsis. Nature Genetics.* **48** (12), 1527-1534 (2016).
15. Phan, M. S. V., Keren, I., Tran, P. T., Lapidot, M., Citovsky, V. *Arabidopsis* LSH10 transcription factor interacts with the co-repressor histone deubiquitinase OTLD1 to recruit it to the target promoters. *bioRxiv.* 10.1101/2022.07.30.502139, (2022).
16. Zhao, L. et al. Overexpression of *LSH1*, a member of an uncharacterised gene family, causes enhanced light regulation of seedling development. *The Plant Journal.* **37** (5), 694-706 (2004).
17. Lei, Y., Su, S., He, L., Hu, X., Luo, D. A member of the *ALOG* gene family has a novel role in regulating nodulation in *Lotus japonicus. Journal of Integrative Plant Biology.* **61** (4), 463-477 (2019).
18. MacAlister, C. A. et al. Synchronization of the flowering transition by the tomato *TERMINATING FLOWER* gene. *Nature Genetics.* **44** (12), 1393-1398 (2012).
19. Takeda, S. et al. CUP-SHAPED COTYLEDON1 transcription factor activates the expression of *LSH4* and *LSH3*, two members of the ALOG gene family, in shoot organ boundary cells. *The Plant Journal.* **66** (6), 1066-1077 (2011).
20. Yan, D. et al. *BEAK-SHAPED GRAIN 1/TRIANGULAR HULL 1*, a *DUF640* gene, is associated with grain shape, size and weight in rice. *Science China Life Sciences.* **56** (3), 275-283 (2013).
21. Yoshida, A. et al. *TAWAWA1*, a regulator of rice inflorescence architecture, functions through the suppression of meristem phase transition. *Proceedings of the National Academy of Sciences.* **110** (2), 767-772 (2013).
22. Yoshida, A., Suzaki, T., Tanaka, W., Hirano, H. Y. The homeotic gene *long sterile lemma (G1)* specifies sterile lemma identity in the rice spikelet. *Proceedings of the National Academy of Sciences.* **106** (47), 20103-20108 (2009).
23. Iyer, L. M., Aravind, L. ALOG domains: provenance of plant homeotic and developmental regulators from the DNA-binding domain of a novel class of DIRS1-type retroposons. *Biology Direct.* **7**, 39 (2012).
24. Peng, P. et al. The rice TRIANGULAR HULL1 protein acts as a transcriptional repressor in regulating lateral development of spikelet. *Scientific Reports.* **7** (1), 13712 (2017).

25. Day, R. N., Periasamy, A., Schaufele, F. Fluorescence resonance energy transfer microscopy of localized protein interactions in the living cell nucleus. *Methods.* **25** (1), 4-18 (2001).

26. Qian, J., Yao, B., Wu, C. Fluorescence resonance energy transfer detection methods: Sensitized emission and acceptor bleaching. *Experimental and Therapeutic Medicine.* **8** (5), 1375-1380 (2014).

27. Campbell, R. E. et al. A monomeric red fluorescent protein. *Proceedings of the National Academy of Sciences.* **99** (12), 7877-7882 (2004).

28. Tzfira, T. et al. pSAT vectors: a modular series of plasmids for fluorescent protein tagging and expression of multiple genes in plants. *Plant Molecular Biology.* **57** (4), 503-516 (2005).

29. Bracha-Drori, K. et al. Detection of protein-protein interactions in plants using bimolecular fluorescence complementation. *The Plant Journal.* **40** (3), 419-427 (2004).

30. Citovsky, V., Gafni, Y., Tzfira, T. Localizing protein-protein interactions by bimolecular fluorescence complementation *in planta. Methods.* **45** (3), 196-206 (2008).

31. Citovsky, V. et al. Subcellular localization of interacting proteins by bimolecular fluorescence complementation *in planta. Journal of Molecular Biology.* **362** (5), 1120-1131 (2006).

32. Ohad, N., Shichrur, K., Yalovsky, S. The analysis of protein-protein Interactions in plants by bimolecular fluorescence complementation. *Plant Physiology.* **145** (4), 1090-1099 (2007).

33. Gookin, T. E., Assmann, S. M. Significant reduction of BiFC non-specific assembly facilitates *in planta* assessment of heterotrimeric G-protein interactors. *The Plant Journal.* **80** (3), 553-567 (2014).

34. Tran, P. T., Citovsky, V. Receptor-like kinase BAM1 facilitates early movement of the *Tobacco mosaic virus. Communications Biology.* **4** (1), 511 (2021).

35. Walhout, A. J. et al. GATEWAY recombinational cloning: application to the cloning of large numbers of open reading frames or ORFeomes. *Methods in Enzymology.* **328**, 575-592 (2000).

36. Ashwini, M., Murugan, S. B., Balamurugan, S., Sathishkumar, R. Advances in molecular cloning. *Molecular Biology.* **50** (1), 1-6 (2016).

37. Tzfira, T. et al. Transgenic *Populus*: a step-by-step protocol for its *Agrobacterium*-mediated transformation. *Plant Molecular Biology Reporter.* **15**, 219-235 (1997).

38. Wise, A. A., Liu, Z., Binns, A. N. Nucleic acid extraction from *Agrobacterium* strains. *Methods in Molecular Biology.* **343**, 67-76 (2006).

39. Bal, M., Zhang, J., Hernandez, C. C., Zaika, O., Shapiro, M. S. Ca2+/calmodulin disrupts AKAP79/150 interactions with KCNQ (M-Type) K+ channels. *The Journal of Neuroscience.* **30** (6), 2311-2323 (2010).

40. Feige, J. N., Sage, D., Wahli, W., Desvergne, B., Gelman, L. PixFRET, an ImageJ plug-in for FRET calculation that can accommodate variations in spectral bleed-throughs. *Microscopy Research & Technique.* **68** (1), 51-58 (2005).

41. Bal, M., Zhang, J., Hernandez, C. C., Zaika, O., Shapiro, M. S. Ca2+/calmodulin disrupts AKAP79/150

interactions with KCNQ (M-Type) K+ channels. *Journal of Neuroscience.* **30** (6), 2311-2323 (2010).

42. Taylor, N. J., Fauquet, C. M. Microparticle bombardment as a tool in plant science and agricultural biotechnology. *DNA and Cell Biology.* **21** (12), 963-977 (2002).
43. Broussard, J. A., Green, K. J. Research techniques made simple: methodology and applications of Förster resonance energy transfer (FRET) microscopy. *Journal of Investigative Dermatology.* **137** (11), e185-e191 (2017).
44. Kudla, J., Bock, R. Lighting the way to protein-protein interactions: recommendations on best practices for bimolecular fluorescence complementation analyses. *The Plant Cell.* **28** (5), 1002-1008 (2016).
45. Bartel, P., Chien, C. T., Sternglanz, R., Fields, S. in *Cellular Interactions in Development: A Practical Approach.* (ed D.A. Hartley). IRL Press. 153-179 (1993).
46. Fields, S., Song, O. A novel genetic system to detect protein-protein interactions. *Nature.* **340** (6230), 245-246 (1989).
47. Phizicky, E. M., Fields, S. Protein-protein interactions: methods for detection and analysis. *Microbiological Reviews.* **59** (1), 94-123 (1995).
48. Fields, S. High-throughput two-hybrid analysis. The promise and the peril. *The FEBS Journal.* **272** (21), 5391-5399 (2005).
49. Azad, T., Tashakor, A., Hosseinkhani, S. Split-luciferase complementary assay: applications, recent developments, and future perspectives. *Analytical and Bioanalytical Chemistry.* **406** (23), 5541-5560 (2014).
50. Wang, L., Yu, G., Macho, A. P., Lozano-Durán, R. Split-luciferase complementation imaging assay to study protein-protein interactions in *Nicotiana benthamiana. Bio-protocol.* **11** (23), e4237 (2021).
51. Grefen, C., Lalonde, S., Obrdlik, P. Split-ubiquitin system for identifying protein-protein interactions in membrane and full-length proteins. *Current Protocols in Neuroscience.* **41** (1), 5-27 (2007).
52. Thaminy, S., Miller, J., Stagljar, I. The split-ubiquitin membrane-based yeast two-hybrid system. *Methods in Molecular Biology.* **261**, 297-312 (2004).
53. Lin, J. S., Lai, E. M. Protein-protein interactions: co-immunoprecipitation. *Methods in Molecular Biology.* **1615**, 211-219 (2017).
54. Jiang, Z., Yang, M., Cao, Q., Zhang, Y., Li, D. A powerful method for studying protein-protein interactions in plants: coimmunoprecipitation (co-IP) assay. *Methods in Molecular Biology.* **2400**, 87-92 (2022).
55. Magori, S., Citovsky, V. *Agrobacterium* counteracts host-induced degradation of its F-box protein effector. *Science Signaling.* **4** (195), ra69 (2011).